Cycle-to-Cycle Transient Model of 4-stroke Combustion Engines

Madan Kumar and Tielong Shen
Department of Engineering and Applied Science, Sophia University, Tokyo, Japan

Keywords: Modeling, Combustion Engines, Discrete-time System.

Abstract: In 4-stroke combustion engines, managing the cycle-to-cycle transient characteristics of the mass of the air, the fuel and the burnt gas is an important issue due to the cycle-to-cycle coupling caused by the imbalance of cyclic combustion. This paper presents a discrete-time model that represents the cycle-to-cycle transient behavior of in-cylinder state variables under the assumption of measurability of the total gas mass and the residual gas fraction. It is shown that if the state variables are chosen as total fuel mass, residual unburnt air and the burnt gas mass, then the system is modeled as a time-varying linear system. Validation results is demonstrated which conducted on a full-scaled gasoline engine test bench.

1 INTRODUCTION

In internal combustion engine, combustion inside the cylinder is a complex phenomena and exhibit substantial cycle-to-cycle variation. This cyclic variation is observed to stochastic in process. Some physical model has been developed to characterized the transient behavior of engine phenomena on cycle basis [(Rizzoni, 1989),(Peyton Jones, 2010)]. This cyclic variation affects the engine performance, such as air-fuel ratio, torque generation and so on. The mainly affecting variables are residual gas, unburned fuel and unburned air succeeding the next cycle from previous cycle. There are so many factors that influence the cyclic residual gas, and it is not feasible to represent the influence mathematically in general. Analysis and research in this area is continue from 19th century (Clerk,1886) and still there is some gap in satisfactory solution. In engine research's, researchers mainly aim to improve the power generation and reduce the emission due to the limitation of sources of fuel and environmental pollution effect. The engine performance goes down with the increases of residual gas in engine cylinder. However it decreases the emission as NOx decreases in cylinder due to in-cylinder temperature decreases.

On another side, a good modeling mechanism of the engine is also a fact to improve the performance of engine. Since the in-cylinder phenomena like in-cylinder air, fuel and residual gas compositions are not measurable directly except to in cylinder pressure, model based observers are thus necessary to estimate these quantities. This ambiguity has created a continuing challenging to find a suitable control model to estimate the true nature of in-cylinder cycle-to-cycle behavior [(Daw, 1996),(Daw, 1998),(Jonathan, 2008),(Yang, 2013)].

In this paper a discrete-time model that represents the cycle-to-cycle transient behavior of in-cylinder state variables under the assumption of measurability of the total gas mass and the residual gas fraction is proposed. The system is modeled as a time-varying linear system as the state variables are chosen as total fuel mass, residual unburnt air and the burnt gas mass.Validation results are demonstrated which conducted on a full-scaled gasoline engine test bench. The detail about the evaluation of total charge and residual gas fraction are discussed in next section.

2 SYSTEM DESCRIPTIONS

As is well known that the in-cylinder gas and combustion phenomena are difficult to measured directly on cycle-to-cycle basis in engine dynamic systems. In internal combustion engines, fuel and air goes inside the engine cylinder and releases heat energy due to the chemical reaction happened between fuel and air and this heat energy is used to convert in mechanical energy to produced the work. In four strokes engine, one cycle includes the suction, compression, combustion and exhaust process. In general, fresh air and fuel mixture enters in cylinder during suction stroke and it compressed during compression in four stroke

Kumar M. and Shen T..
Cycle-to-Cycle Transient Model of 4-stroke Combustion Engines.
DOI: 10.5220/0005095107450750
In *Proceedings of the 4th International Conference on Simulation and Modeling Methodologies, Technologies and Applications* (SIMULTECH-2014), pages 745-750
ISBN: 978-989-758-038-3

gasoline engine. For the start of combustion, spark is generated 30 to 40 deg. before top dead centre (TDC) which depends upon the engine configuration and power required. In combustion stroke due to high pressure and temperature inside the cylinder, piston pushed out towards bottom dead centre (BDC) by the in-cylinder high pressure and temperature charge and hence power transfered to crank shaft. At the end of combustion stroke, the exhaust valve open and exhaust gas expelled due to the high pressure of gas inside the cylinder. In advance research, the direct injection gasoline is used for improved the combustion phenomena and performance of engines in which gasoline is direct injected in port or in cylinder which is named as gasoline direct injection (GDI) engine. Due to the limitation in engine design, the exhaust gas in one cycle does not expelled fully during the exhaust stroke and it remains for the next cycle which affects the combustion in next cycle. The engine performance is affected due to this remained gas in cylinder.

In engine, variable valve timing (VVT) system, engine speed and load also affects the cycle to cycle variation. A schematic diagram of experimental setup with VVT control system is shown in Fig.1. A gasoline 3.5L engine is used for the experiment which is supported by Toyota Motors Corporation (Fig.2). This engine having port and direct injection system and engine is well instrumented to get almost full data to analyze the engine behavior. In this engine, VVT system is also in-build for the analysis of the effects of VVT on in-cylinder gas contains during cycle-to-cycle fluctuation. For control and capturing the data, ECU and dSPACE are used.

In this experimental test bench, experiment is conducted for the measurement of total charge and residual gas estimation on the cycle basis keeping the fixed spark advance and torque and varying the VVT. The variation in the magnitude of total charge and residual gas is observed to fluctuate on cycle to cycle basis. A sample of variation in residual gas fraction (RGF) on cycle basis is shown in Fig.3. From figure 3, it is observed that the cyclic variation of residual gas fraction is in stochastic process which cannot be predicted easily for the next cycle.

The total charge is calculated in compression stroke before start of combustion and residual gas fraction (RGF) at the end of exhaust stroke on cycle to cycle basis. The total charge in-cylinder can be calculated by two method. (a). Using the direct measurement of fresh inducted air, fresh injected fuel and estimated RGF using pressure sensor. (b). Using the in-cylinder pressure data. The total charge estimated by direct measurement of fresh inducted air, fuel injected and RGF is as given below,

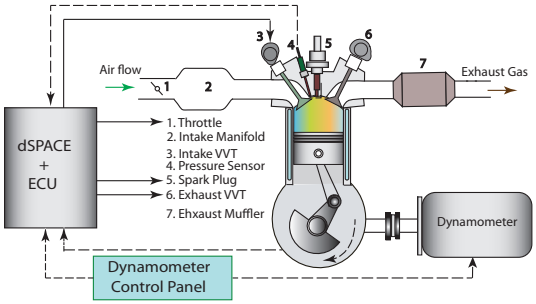

Figure 1: Schematic diagram of experimental setup.

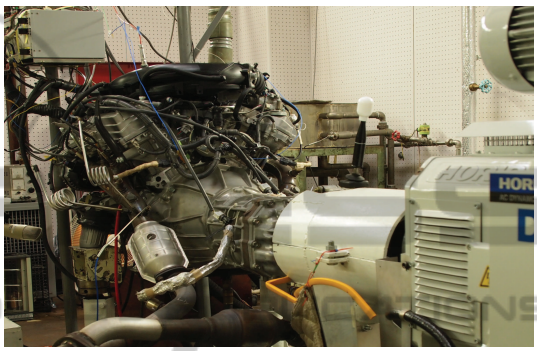

Figure 2: Engine Setup.

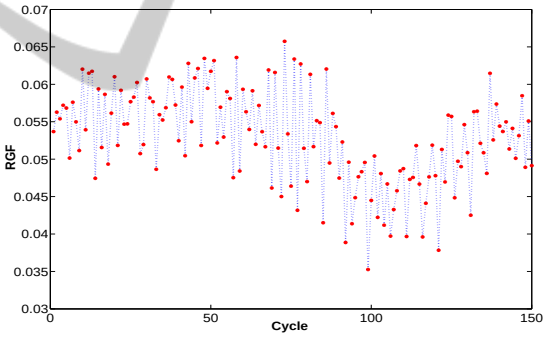

Figure 3: Cyclic residual gas fraction (RGF) sample.

$$M_{ts}(k) = \frac{m_{ind}(k-1) + m_{fn}(k-1)}{(1-r(k))} \quad (1)$$

where $m_{ind}(k-1)$ and $m_{fn}(k-1)$ are the fresh inducted air charge and injected fuel respectively from the previous cycle for the combustion of present cycle on the basis of cycle definition as shown in Fig.5.

In the second method, total charge is calculated using the in-cylinder pressure data [(Arsie, 2013),(Desantes, 2010)] as given below,

$$M_{tp}(k) = \frac{\Delta P(k) V_1(k)}{R T_1(k)} \{ (\frac{V_1(k)}{V_2(k)})^n - 1 \}^{-1} \quad (2)$$

where ΔP is the difference of pressure $P_2(k)$ and $P_1(k)$.

Similarly, the residual gas fraction r(k) at the end of exhaust stroke can also be calculated using in-cylinder pressure data as given in equation 3 (Yang, 2013). A figure for suitable measurement points for pressure and volume is shown in Fig.4.

$$r(k) = \frac{M_r(k)}{M_t(k)} = (\frac{V_4(k)}{V_3(k)})(\frac{P_4(k)}{P_3(k)})^{\frac{1}{n}} \quad (3)$$

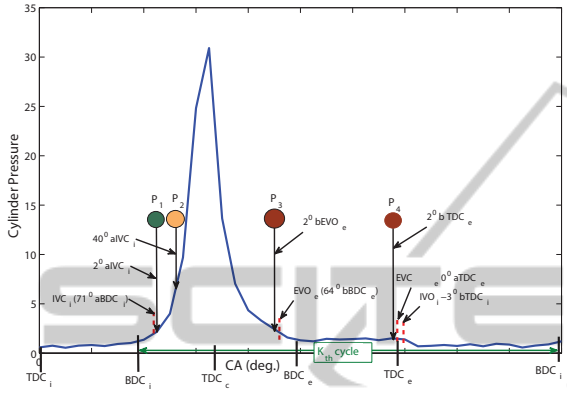

Figure 4: Pressure measurement points indication in pressure vs crank angle plot.

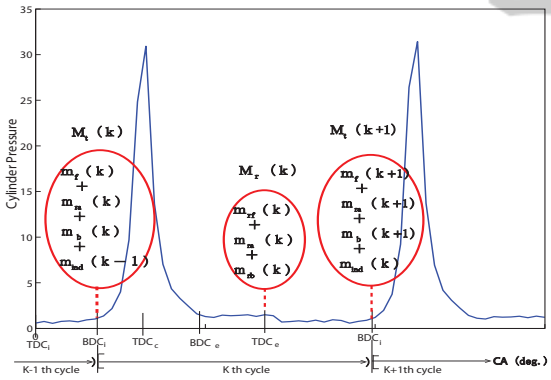

Figure 5: Gas exchange phenomena between cycle.

3 MODELING

For the development of model, cycle is defined from BDCi (k) to BDCi(k+1) as kth cycle in which data at BDCi (k) is included in k_{th} cycle and data at BDCi (k+1) is included in $k+1_{th}$ cycle as shown in Fig.5. In this model, next cycle ($k+1_{th}$ cycle) variables can be estimated using the present cycle (k_{th} cycle) variables using the input control as fresh fuel injection u_f. From Fig.5, It can be observe that the total mass of charge $M_t(k)$ including fresh charge of present cycle and residual gas mass, unburned air and fuel mass from previous cycle will be involved for the present cycle combustion process. A cyclic representation of gas exchange phenomena during cycle to cycle and in cycle is shown in Fig.5.

According to cycle definition as shown in Fig.5 and with the assumptions of mass conservation during the gas exchange in cycle to cycle process, the total mass of fuel, mass of unreacted air (residual air) and residual burned gas present for the combustion in $k+1_{th}$ cycle is derived as,

a). The total mass of fuel available at the start of combustion for $k+1_{th}$ cycle is equal to the summation of mass of unreacted fuel in k_{th} cycle and fresh fuel injected in k_{th} cycle as cycle definition. In mathematical form, the equation can be represented as,

$$\begin{aligned} m_f(k+1) &= m_{fur}(k) + m_{fn}(k) \\ &= (1 - C_f(k)(r(k))m_f(k) + u_f(k) \end{aligned} \quad (4)$$

b). The unreacted air (residual air) at the start of combustion in $k+1_{th}$ cycle is equal to the residual air which is remained at the end of k_{th} cycle and represented as,

$$\begin{aligned} m_{ra}(k+1) &= r(k)\{[m_{ra}(k) + m_{ind}(k-1)] \\ &\quad -\lambda_d C_f(k) m_f(k)\} \\ &= r(k)m_{ra}(k) - \lambda_d r(k) C_f(k) m_f(k) \\ &\quad + r(k) m_{ina}(k-1) \end{aligned} \quad (5)$$

c). The burned gas at the start of combustion in $k+1_{th}$ cycle is equal to the residual burned gas at the end of k_{th} cycle and is represented as,

$$\begin{aligned} m_b(k+1) &= r(k)[m_b(k) + C_f(k) m_f(k) \\ &\quad + \lambda_d C_f(k) m_f(k)] \\ &= r(k) m_b(k) \\ &\quad + r(k) C_f(k)(1+\lambda_d) m_f(k) \end{aligned} \quad (6)$$

And total mass of charge $M_t(k)$ before start of combustion in kth cycle assuming mass conservation during process is as,

$$M_t(k) = m_f(k) + m_{ra}(k) + m_b(k) + m_{ind}(k-1) \quad (7)$$

where, $m_f(k)$ is the total mass of fuel $(= m_{fn}(k) + m_{fur}(k-1))$ available in the cylinder at the start of combustion, m_{fur} is unreacted fuel from previous cycle which is available for the combustion in present cycle, C_f is the combustion efficiency, $(u_f(k) = m_{fn}(k))$ is fresh fuel injected, $r(k)$ is residual gas fraction(RGF), m_{ra} is unreacted air mass, λ_d is the stoichiometric air fuel ratio, $m_{ind}(k-1)$ is fresh air inducted in cylinder during suction stroke and m_b is burned gas mass.

For the sake of simplicity, the assumptions for $C_f(k)$ and $r(k)$ variations for the simulation are considered as,

1). $C_f(k) = C_0\ (1+\sigma(k)) = C_0 + e(k)$, $e(k) \in N(0, \sigma^2)$

2). $r(k)$ is measurable using equation 3 and a distribution sample is given in below Fig 6.

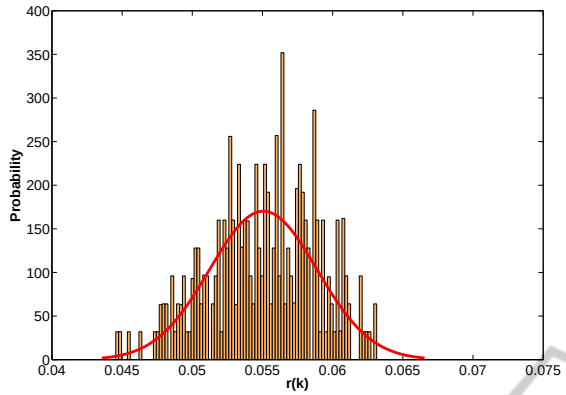

Figure 6: r(k) distribution sample.

where, e(k) is the variance of the distribution.

Equation number 4, 5 and 6 can be written in matrix form as given below,

$$\begin{bmatrix} m_f(k+1) \\ m_{ra}(k+1) \\ m_b(k+1) \end{bmatrix} = \begin{bmatrix} (1-C_f(k))r(k) & 0 & 0 \\ -\lambda_d r(k) C_f(k) & r(k) & 0 \\ r(k)C_f(k)(1+\lambda_d) & 0 & r(k) \end{bmatrix} \begin{bmatrix} m_f(k) \\ m_{ra}(k) \\ m_b(k) \end{bmatrix} + \begin{bmatrix} 1 \\ 0 \\ 0 \end{bmatrix} u_f(k) + \begin{bmatrix} 0 \\ r(k) \\ 0 \end{bmatrix} (\Delta + \zeta(k)) \tag{8}$$

For the modeling and control systems, two assumptions are consider as follows,

1). $m_{ind}(k-1) = \Delta + \zeta(k)$

2). $y(k) = M_t(k) - \Delta$

where, $y(k)$ = $\Sigma x(k)$, Δ is constant and assumed to measurable (= $m_{ind}(k-1)$), $\zeta(k)$ is variance ($\zeta(k) \in N(0, \sigma^2)$.

Then finally from equation 8, the discrete time model for estimation of cycle to cycle behaviors and its control is represented as,

$$x(k+1) = A(k)x(k) + B_1 u_f(k) + B_2(k)(\Delta + \zeta(k)) \tag{9}$$

$$y_{mod}(k) = Cx(k) + \zeta(k) \tag{10}$$

where $x(k)$ is the state variables and $A(k)$, $B_1(k)$,$B_2(k)$ and C are constants as given below,

$$x(k) = \begin{bmatrix} m_f(k) \\ m_{ra}(k) \\ m_b(k) \end{bmatrix}, C = \begin{bmatrix} 1 & 1 & 1 \end{bmatrix},$$

$$A(k) = \begin{bmatrix} (1-C_f(k))r(k) & 0 & 0 \\ -\lambda_d r(k) C_f(k) & r(k) & 0 \\ r(k)C_f(k)(1+\lambda_d) & 0 & r(k) \end{bmatrix},$$

$$B_1 = \begin{bmatrix} 1 \\ 0 \\ 0 \end{bmatrix} \text{ and } B_2(k) = \begin{bmatrix} 0 \\ r(k) \\ 0 \end{bmatrix}$$

4 VALIDATION

Validation of model is done on the static state using fixed input and variables and also on the actual experimental data. The influence of variables are also found out in this section adding some noise in fixed input variables and parameters.

4.1 Simulation Results

In this case, initially fixed input data is used for the validation of model is as, $C_f(k)$ = 0.8 , $r(k)$ = 0.1, Δ =15 mg, $u_f(k)$ = Δ/14.6 and $x(0)$ = $\begin{bmatrix} 1 & 1.5 & 0.8 \end{bmatrix}^T$.

Using the above initial input data in model, the equilibrium points of initial value of $x(0)$ are calculated by simulation and thereafter this equilibrium data is used as initial value of $x(0)$ for further analysis.

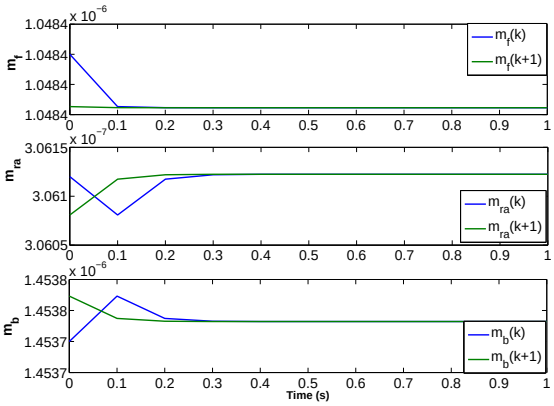

Figure 7: x(k) and x(k+1).

A variation in state variables $x(k)$ and $x(k+1)$ are shown in Fig.7. In this graph, it can be observe that the both signals are able to merged after some delay of time during simulation. The input signal $C_f(k)$ and $r(k)$ have added 20 percent noise in signal and also input value of $u_f(k)$ is changed by magnitude of 15 percent for 10 second during the simulation time for the observing the influence of fuel injection on $x(k)$ and $y(k)$. The result is as shown in Fig.8. From figure, it can be seen that due to changes of $u_f(k)$, $m_f(k)$

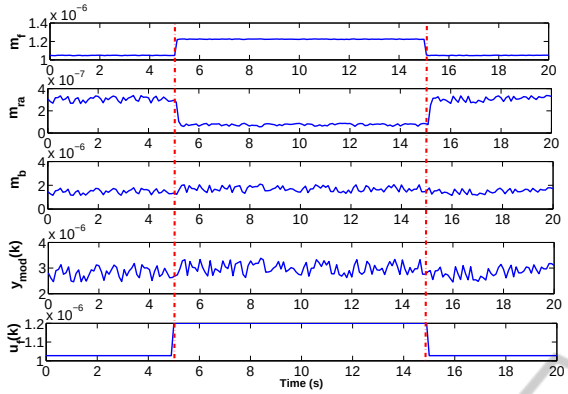

Figure 8: Influence of $u_f(k)$ on x(k) and y(k).

and $m_{ra}(k)$ are changes significantly but there are less influence on $m_b(k)$ and $y_{mod}(k)$ is noted.

4.2 Experimental Validation

For the model validation in realistic condition of engine behavior, the experimental data of RGF and total charge from engine experiment are used for simulation. The value of $y(k)$ calculated from the model and from the engine data are compared in this section. A block diagram of simulation is shown in Fig.9. From the block diagram, it can be seen that the m_{ind} and u_f are the input variables for the engine and simulation both. From simulation, we can find the value of $y_{mod}(k)$ using the RGF data from the engine experiment. On another side, the $y_{cal}(k)$ can also be calculated from the engine experimental data.

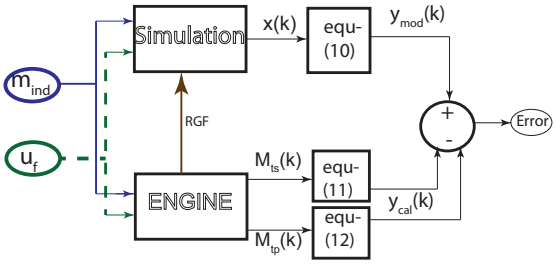

Figure 9: Block diagram of simulation.

4.2.1 Validation using $M_{ts}(k)$

In this case, $y_{cal}(k)$ is calculated using the below given formula and compared with the $y_{mod}(k)$ model,

$$y_{cal}(k) = M_{ts}(k) - \Delta \tag{11}$$

where $M_{ts}(k)$ can be calculated using equation (1) and Δ can be measured by sensor. A comparison graph of $y_{cal}(k)$ and $y_{mod}(k)$ is shown in Fig.10. From graph

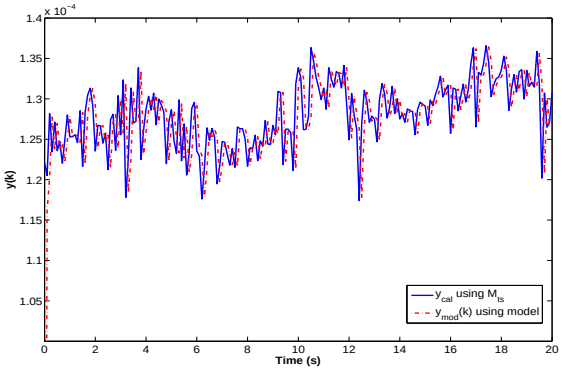

Figure 10: $y_{cal}(k)$ and $y_{mod}(k)$.

it can be observed that the $y_{cal}(k)$ and $y_{mod}(k)$ are approximately equal after some delay of simulation cycle.

4.2.2 Validation using $M_{tp}(k)$

In this case, $y_{cal}(k)$ is calculated using the below given formula and compared with the $y_{mod}(k)$ model,

$$y_{cal}(k) = M_{tp}(k) * r(k) + m_{fn}(k-1) \tag{12}$$

where $M_{tp}(k)$ can be calculated using equation (2). A comparison graph of $y_{cal}(k)$ and $y_{mod}(k)$ is shown in Fig.11. Form this graph it can be observed that the error between $y_{cal}(k)$ and $y_{mod}(k)$ is more compared to previous method which is due to the propagation of error in $M_{tp}(k)$, r(k) and $m_{fn}(k-1)$ measured by the pressure and fuel sensors.

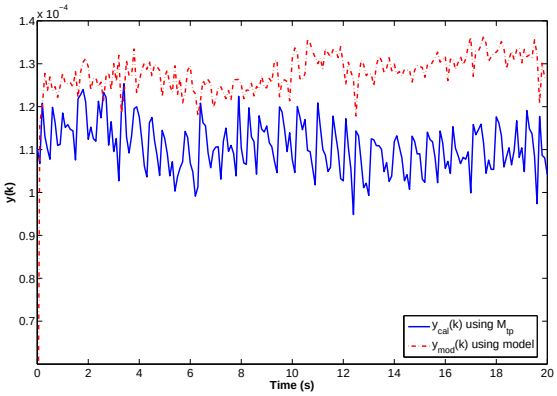

Figure 11: $y_{cal}(k)$ and $y_{mod}(k)$

The distribution of y_{cal} for the simulation time of 20 second are plotted in Figures 12 ,13 and 14. In figures 12 and 14, the distribution of y_{cal} measured by M_{ts} and y_{mod} respectively is plotted in which mean

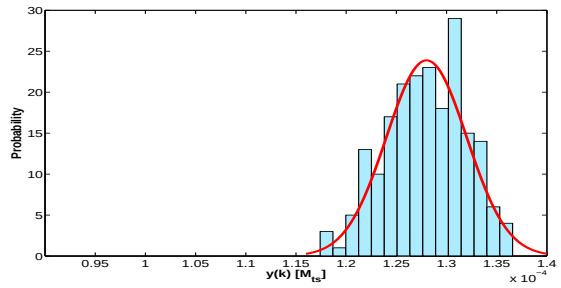

Figure 12: Probability distribution of $y_{cal}(k)$ using M_{ts}.

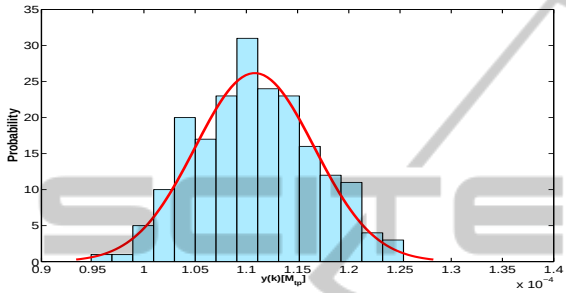

Figure 13: Probability distribution of $y_{cal}(k)$ using M_{tp}.

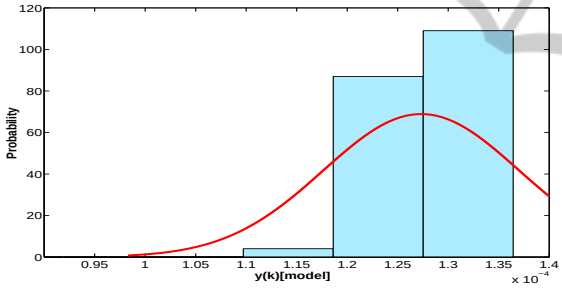

Figure 14: Probability distribution of $y_{mod}(k)$ using model.

value of data distribution seems to be equal. That shows the model and experimental results are seems to be satisfactory. In figures 12 and 13, the distribution of y_{cal} measured by M_{tp} and y_{mod} are observed to be different mean value.

5 CONCLUSIONS

A discrete-time model is developed and validated with the static and transient mode. The model is also validated using the real engine experimental data. The y(k) calculated using the two methods of total charge estimation and y (k) from model are compared. The error in y(k) in case of $M_{tp}(k)$ is higher than the calculated by $M_{ts}(k)$ due to the propagation of error in different measured variables. In further continuing of this research work, validation of model will be done based on the $y(k)$ measured using M_{tp} by the adding of some correction factor to minimized the error at different operating condition of engine data. A observer will be established to control the air-fuel ratio, torque and RGF using above model on cycle basis.

ACKNOWLEDGEMENTS

The authors wish to acknowledge the Toyota Motors Corporation for the supporting in this research and helpful discussions and Mr. Mingxin Kang for the helping in conduct the experiment:

REFERENCES

Rizzoni G. (1999). A stochastic model for the indicated pressure process and the dynamics of internal combustion engine. *IEEE Trans. Veh. Technol.*, vol.38, no. 3, pp.180-192, Aug. 1989.

Peyton Jones, J. C., Roberts J. B., and Landsborough K.J. (2010). A cumulative-summation-based stochastic knock controller. *Proc. Inst. Mech. Eng.*, vol.224, no. 7, pp. 969-983, 2010.

Clerk, D. (1886). The gas engine. *1st ed., Longmans, Green and Co.*, 1886.

Daw, C. S., Finney, C. E. A., Green, J. B., Kennel, M. B., and Thomas, J. F. (1996). A simple model for cyclic variations in a spark-ignition engine. *SAE Warrendale, PA*,.962086, May 1996.

Daw, C. S., Finney, C. E. A., Kennel, M. B., and Connolly, F. T. (1998). Observing and modeling nonlinear dynamics in an internal combustion engine. *Phys. Rev. E.*, vol.57, no.3, pp. 2811-2819, 1998.

Arsie, I., Rocco, D., L., Pianese, C., and Cesare, M., D. (2013). Estimation of in-cylinder mass and AFR by cylinder pressure measurement in automotive Diesel engines. *IFAC World Congress*, 2013.

Desantes, J. M., Galindo, J., Guardiola, C., and Dolz, V. (2010). Air mass flow estimation in turbocharged diesel engines from in-cylinder pressure measurement. *Experimental Thermal and Fluid Science*, vol. 34, pp. 37-47, 2010.

Yang, J., Shen, T., and Jiao, X. (2010). Model-based stochastic optimal air-fuel ratio control with Residual gas fraction of spark ignition engine *IEEE*, 2013.

Jonathan, B. V., Brian, C. K., Jagannathan, S., and Drallmeier, J.,M (2008). Optput feedback controller for operation of spark ignition engines at lean conditions using neural networks. *IEEE*, vol. 16, no. 2, March 2008.